

DESIGN OF A SHIPPING FIXTURE FOR A COMPACT CRYOMODULE HERMETIC ASSEMBLY

J. Lewis^{1,†}, G. Ciovati^{1,2,3}, N. Huque², J. Armstrong², K. Harding²

¹Mechanical and Aerospace Engineering, Old Dominion University, Norfolk, VA, USA

²Jefferson Lab, Newport News, VA, USA

³Center for Accelerator Science, Old Dominion University, Norfolk, VA, USA

Abstract

Two conduction-cooled 915 MHz superconducting radio frequency hermetic assemblies must be safely transported from the Jefferson Lab in Newport News, VA to General Atomics in San Diego, CA for performance testing in a custom horizontal test cryostat. One hermetic assembly consists of a 2-cell 915 MHz cavity, a coaxial fundamental power coupler, and the warm-to-cold transition beam tubes. The second hermetic assembly consists of a 2-cell 915 MHz cavity only. The assemblies will be transported on a flatbed air-ride trailer over the approximate 4000 km distance. Design requirements included adequate attenuation of 4g vertical axis, 5g beamline axis, and 1.5g lateral axis shock events. The isolation system was designed using helical wire-rope isolators with modal and transient finite element analysis performed in Ansys. Results show shock attenuation of a 10 ms half-sine pulse input to < 1g in the vertical axis, < 1.5g in the beamline axis, and < 0.5g in the lateral axis for both assemblies at the specified design loads and all structural stresses are kept below the material yield limits. Additionally, the natural frequencies of both isolation systems adequately attenuate the fundamental modes of the critical structures.

INTRODUCTION

In support of the development of a conduction-cooled 915 MHz superconducting radio frequency (SRF) cryomodule, this study highlights the development of a shipping fixture for transporting two separate hermetic assemblies, shown in Fig. 1, approximately 4000 km from Jefferson Lab in Newport News, VA to General Atomics in San Diego, CA via a flatbed air-ride trailer. Transportation exposes the assemblies to vibrational and shock environments which pose significant risk of damage if not properly isolated [1]. The design requirements set by Jefferson Lab include adequate attenuation of 5g shock loads in the beamline direction, 4g vertical, and 1.5g such that shock-induced stresses are kept sufficiently below material yield limits. Additionally, the fundamental mode of the isolation system must account for the natural frequencies of the ground transportation vehicle and all critical structures in the hermetic assemblies to prevent vibrational-induced damage. Critical components include the Nb cavities, the Cu antenna of the fundamental power coupler (FPC), and the FPC Al ceramic window. The inner surfaces of both

cavities will be coated in Nb₃Sn at 1200 °C for 6 h, reducing the yield of the Nb to ~31 MPa. The Nb₃Sn layer has shown to be easily damaged when the Nb substrate undergoes any plastic deformation. To ensure this does not occur, the stress limit for both cavities was set at ≤15.5 MPa, half of the estimated yield strength [2]. The high purity Cu antenna of the FPC has a yield of ~33 MPa and the Al ceramic window has a flexural strength of ~296 MPa [3].

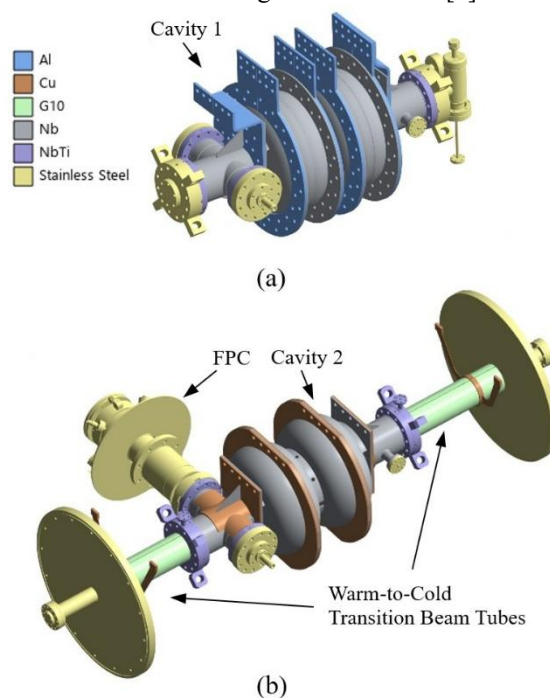


Figure 1: (a) The hermetic assembly consisting of an SRF cavity only. (b) The hermetic assembly consisting of an SRF cavity, coaxial FPC, and warm-to-cold transition beam tubes. The Cu antenna and Al ceramic window are housed within the FPC.

SHIPPING FIXTURE DESIGN

The shipping fixture consists of two primary structures, an outer and inner frame. The hermetic assembly is mounted to the inner frame while the outer frame is mounted to the trailer of the transporting truck. The two frames are then connected through helical wire-rope isolators. The non-linear stiffness characteristics of these isolators provides unique vibrational, K_v , and shock, K_s , spring-rates for six different loading orientations, making them a cost-effective and versatile isolation device. The wound stainless-steel cables provide energy dissipation resulting

* Work supported by the U.S. DOE Office of Accelerator R&D and Production and the Office of Nuclear Physics through Jefferson Science Associates, LLC under U.S. DOE Contract No. DE-AC05-06OR23177.

† jacobl@jlab.org

in damping ratios, $\frac{c}{c_c}$, of 0.2 for vibration and 0.15 for shock events [4]. A primary universal inner frame measuring 1.34 m x 0.45 m x 0.45 m made from titanium is used for both hermetic assemblies and provides mounting of all Al 7075 support structures including the isolator attachment frame.

The isolator attachment bars are centered at the structures center of gravity and provide mounting of up to three wire-rope isolators on each side of the assembly in a 45° load bearing orientation. The inner frame assembly 1, shown in Fig. 2(a) utilizes four total isolators, while assembly 2, shown in Fig. 2(b) utilizes six.

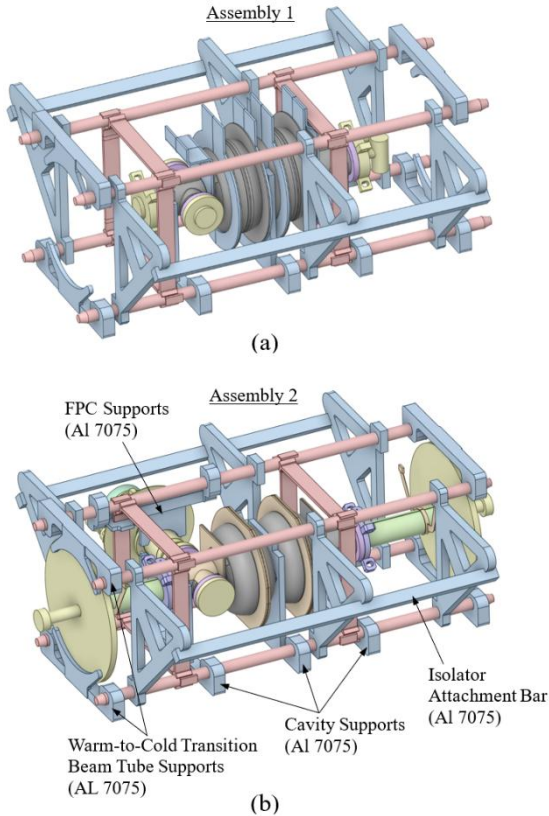


Figure 2: (a) Inner frame assembly 1, mass ~136 kg, 4 isolators. (b) Inner frame assembly 2, mass ~205 kg, 6 isolators.

Modal analysis was performed in Ansys to determine the fundamental modes of both assemblies as well as the cavities and FPC antenna and the results are shown in Table 1. A target natural frequency range of 7-10 Hz for both systems was then determined using a power spectral density curve (PSD) for air-ride suspension [5]. This provides > 90% attenuation to all fundamental modes of the critical components, while avoiding peaks in the PSD curve. The system is modeled as undamped, single degree of freedom along each axis to determine the required isolator spring-rates, given by

$$f_n = \frac{1}{2\pi} \sqrt{\frac{K_v \cdot n}{m}} \quad (1)$$

where f_n is the resulting natural frequency of the system, n is the number of isolators, and m is the total mass of the inner frame assembly.

Table 1: Modal Analysis Results

Component	f_n [Hz]
Assembly 1	67.9
Cavity 1	176.8
Assembly 2	73.5
Cavity 2	125.6
FPC Antenna	114

The transportation shock events are modeled as half-sine pulse inputs [6,7]. Accelerometer data from previous transportation projects at Jefferson Lab indicate a pulse duration of 0.01 s to 0.03 s for all significant events >1g [8]. Analysis of a half-sine pulse acceleration and pseudo-velocity shock response spectrum curves show that longer duration, lower frequency shock events are more difficult to attenuate due to the rigid behavior they induce in the system response while shorter duration, higher frequency events have greater potential to induce higher stresses at equivalent system response frequencies [6, 7]. Half-sine pulse durations of 0.01 s, 0.02 s, and 0.03 s, corresponding to shock input frequencies, f_i , of 50 Hz, 25 Hz, and 16.7 Hz were considered for the design. The system response frequency is given by:

$$f_o = \frac{1}{2\pi} \sqrt{\frac{K_s \cdot n}{m}} \quad (2)$$

It can be found that this commonly leads to frequency ratios of system response-to-shock input < 0.5. In this range, a normalized shock response spectrum with a damping ratio of 0.15 shows an approximate relationship for the system's response as

$$\ddot{x}_o = 1.6 \ddot{x}_i \frac{f_o}{f_i} \quad (3)$$

where \ddot{x}_o is the acceleration response and \ddot{x}_i is the peak shock input. The wire-rope isolators were then selected to minimize the acceleration response at the prescribed shock loads and frequencies, while maintaining the desired system natural frequency of 7-10 Hz and ensuring adequate room for the dynamic deflection as estimated by:

$$\delta_{deflection} = \frac{m \cdot g \cdot \ddot{x}_o}{K_s \cdot n} \quad (4)$$

The selected isolators are P/N: SB22-510-04 from Isolation Dynamics Corporation.

SIMULATION ANALYSIS

Due to computational limitations and the size of the assembly models, the finite element analysis was split into two parts. First, a dynamic response analysis was performed in Ansys by modeling each assembly as a free body

and modeling the wire-rope isolators as bushing contacts to allow for anisotropic spring behaviour as shown in Fig 3. The directional spring-rates were taken directly from the isolator data sheets and the damping coefficients, C , were approximated as viscous damping given by:

$$C = 0.15 \cdot 2 \sqrt{K_s \cdot n \cdot m}. \quad (5)$$

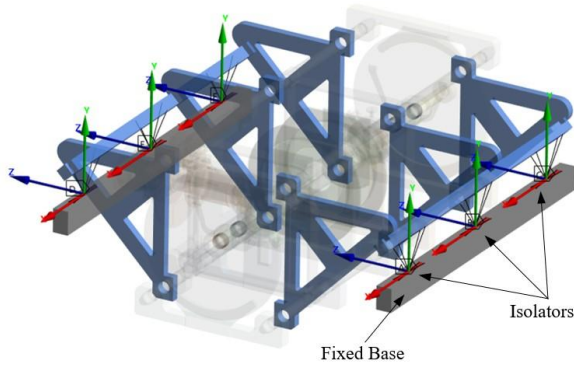


Figure 3: Assembly 2 dynamic response FEA model containing 6 isolators modelled as bushing contacts.

All bodies were meshed with quadratic tetrahedral elements. Peak responses for each design load are shown in Table 2. These responses were then inputted into a transient structural analysis in which the assemblies were fixed at the isolator attachment points, providing the shock-induced stress data for the components. This was found to significantly reduce the computation time when compared to a single full transient analysis. In each case, the stresses found on the primary inner frame and support structures were well below the material yield strengths. Additionally, the maximum stresses on the FPC window and on the stainless-steel bellows of assembly 2 are found to be < 10 MPa and < 80 MPa, respectively. The stresses found on the inner surfaces of both cavities as well as those found on the FPC antenna were of most interest and can be found on Table 3. Both cavities were initially designed to withstand the full undamped prescribed shock loads under static loading conditions. While the static loading condition mitigates transient inertial effects, it was known that an isolation system would be later designed to reduce those peak loads and provided a good baseline design for each cavity as can be seen by the stress results in Table 3. Figure 4 depicts the worst-case stresses found for cavity 1 at a 5g, 30 ms pulse beamline shock load. A modal analysis was performed on the assemblies which included the bushing-modelled isolators shown in Fig. 3. For both assemblies, the f_n along each axis was found to be ~ 7.1 Hz beamline, ~ 8.8 Hz lateral, and ~ 9 Hz vertical, all lying within the targeted frequency range of 7-10 Hz.

Table 2: Transient Responses

Shock Input	Pulse Duration [s]	Assembly 1 Response [g]	Assembly 2 Response [g]
Beamline, 5g	0.01	1.2	1.4
	0.02	2.4	2.5
	0.03	3.3	3.4
Vertical, 4g	0.01	0.8	0.8
	0.02	2.0	2.1
	0.03	3.2	3.3
Lateral, 1.5g	0.01	0.4	0.5
	0.02	0.8	0.9
	0.03	1.1	1.1

Table 3: Shock-Induced Stresses

Shock Input	Pulse Duration [s]	Cavity 1 [MPa]	Cavity 2 [MPa]	FPC Antenna [MPa]
Beamline, 5g	0.01	13.4	11.6	15.9
	0.02	14.1	12.2	19.1
	0.03	14.3	13.1	21.1
Vertical, 4g	0.01	12.2	12.3	15.1
	0.02	13.7	12.8	18.6
	0.03	13.9	13.4	20.2
Lateral, 1.5g	0.01	10.1	10.9	11.9
	0.02	11.2	11.4	12.3
	0.03	11.9	11.6	13.7

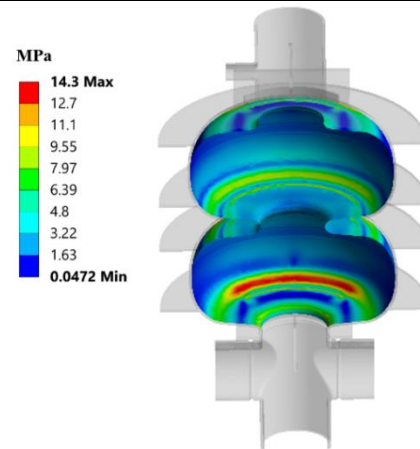


Figure 4: Stresses found on the inner surfaces of cavity 1 of assembly 1 at the 3.3g, 30 ms pulse beamline response load.

CONCLUSION

A satisfactory shipping fixture for both hermetic assemblies has been designed with simulation results showing adequate attenuation of all expected loads. Accelerometer data is planned to be collected during transit to analyse the performance of the systems and provide further information for future designs.

REFERENCES

- [1] N. A. Huque, E. Daly, B. D. Hartsell, J. P. Holzbauer, and P. D. Owen, “Improvements to LCLS-II Cryomodule Transportation,” in *Proc. SRF'19*, Dresden, Germany, Jun.-Jul. 2019, pp. 684-689.
[doi:10.18429/JACoW-SRF2019-TUP094](https://doi.org/10.18429/JACoW-SRF2019-TUP094)
- [2] G. Ciovati, A. Castilla-Loeza, G. Cheng, K. Harding, J. Henry, J. Vennekate, J. Lewis, J. Rathke, and T. Schultheiss, “RF and mechanical design of a 915 MHz SRF cavity for conduction-cooled cryomodes,” in *Proc. LINAC'24*, Chicago, IL, USA, Aug. 2024, pp. 732-735.
[doi:10.18429/JACoW-LINAC2024-THPB046](https://doi.org/10.18429/JACoW-LINAC2024-THPB046)
- [3] S. Thielk *et al.*, “Design of a 25 kW fundamental power coupler for conduction cooled Nb3Sn industrial linac,” in *Proc. LINAC'24*, Chicago, IL, USA, Aug. 2024, pp. 526-529.
[doi:10.18429/JACoW-LINAC2024-TUPB100](https://doi.org/10.18429/JACoW-LINAC2024-TUPB100)
- [4] IDC Isolator, “Wire Rope Isolators,” IDC Isolator, <https://isolator.com/wire-rope-isolators/>.
- [5] International Safe Transit Association, *ISTA 3H: Packaged-Products in Mechanically Handled Bulk Transport Containers*, ISTA, East Lansing, MI, USA, Jan. 2025.
- [6] C. Lalanne, *Mechanical Shock: Mechanical Vibration and Shock Analysis*, 3rd ed., vol. 2. London, U.K.: ISTE Ltd., and Hoboken, NJ, USA: John Wiley & Sons, 2014. ISBN: 978-1-84821-645-7.
- [7] C. M. Harris and A. G. Piersol, *Harris' Shock and Vibration Handbook*, 5th ed. New York, NY, USA: McGraw-Hill, 2002. ISBN: 0-07-137081-1.
- [8] N. Huque, “Shock and alignment analysis of LCLS-II prototype CM during shipping from JLab to FNAL,” TJNAF, Newport News, VA, USA, Internal Report, Aug. 2017.